

## Article

# The Effect on Energy Efficiency of Yttria-Stabilized Zirconia on Brass, Copper and Hardened Steel Nozzle in Additive Manufacturing

Hasan Demir \*  and Atıl Emre Cosgun

Software Engineering Department, The Faculty of Engineering, Aksaray University, Aksaray 68300, Turkey; atilemrecosgun@aksaray.edu.tr

\* Correspondence: hasandemir@aksaray.edu.tr

**Abstract:** This study aimed to investigate if a thermal barrier coating (TBC) affected the energy efficiency of 3D printers. In accordance with this purpose, the used TBC technique is clearly explained and adapted to a nozzle in a simulation environment. Brass, copper, and hardened steel were selected to be the materials for the nozzles. The reason for the usage of a thermal barrier coating method is that the materials are made with low thermal conductivity, which reduces the thermal conductivity and energy losses. Yttria-stabilized zirconia was used to coat material on brass, copper, and hardened steel. To prevent temperature fluctuations, yttria-stabilized zirconia together with a NiCrAl bond layer was used and, thus, heat loss was prevented. Additionally, the paper addressed the effects of the coating on the average heat flux density and the average temperature of the nozzles. In addition, by means of the finite element method, steady-state thermal analyses of the coated and uncoated nozzles were compared, and the results show that the thermal barrier coating method dramatically reduced energy loss through the nozzle. It was found that the average heat flux was reduced by 89.4223% in the brass nozzle, 91.6678% in the copper nozzle, and 79.1361% in the hardened steel nozzle.



**Citation:** Demir, H.; Cosgun, A.E. The Effect on Energy Efficiency of Yttria-Stabilized Zirconia on Brass, Copper and Hardened Steel Nozzle in Additive Manufacturing. *Coatings* **2022**, *12*, 690. <https://doi.org/10.3390/coatings12050690>

Academic Editor: Manuela Ferrara

Received: 6 April 2022

Accepted: 15 May 2022

Published: 17 May 2022

**Publisher's Note:** MDPI stays neutral with regard to jurisdictional claims in published maps and institutional affiliations.



**Copyright:** © 2022 by the authors. Licensee MDPI, Basel, Switzerland. This article is an open access article distributed under the terms and conditions of the Creative Commons Attribution (CC BY) license (<https://creativecommons.org/licenses/by/4.0/>).

**Keywords:** energy efficiency; NiCrAl; yttria-stabilized zirconia; 3D printer; brass; copper; hardened steel nozzle; finite element method

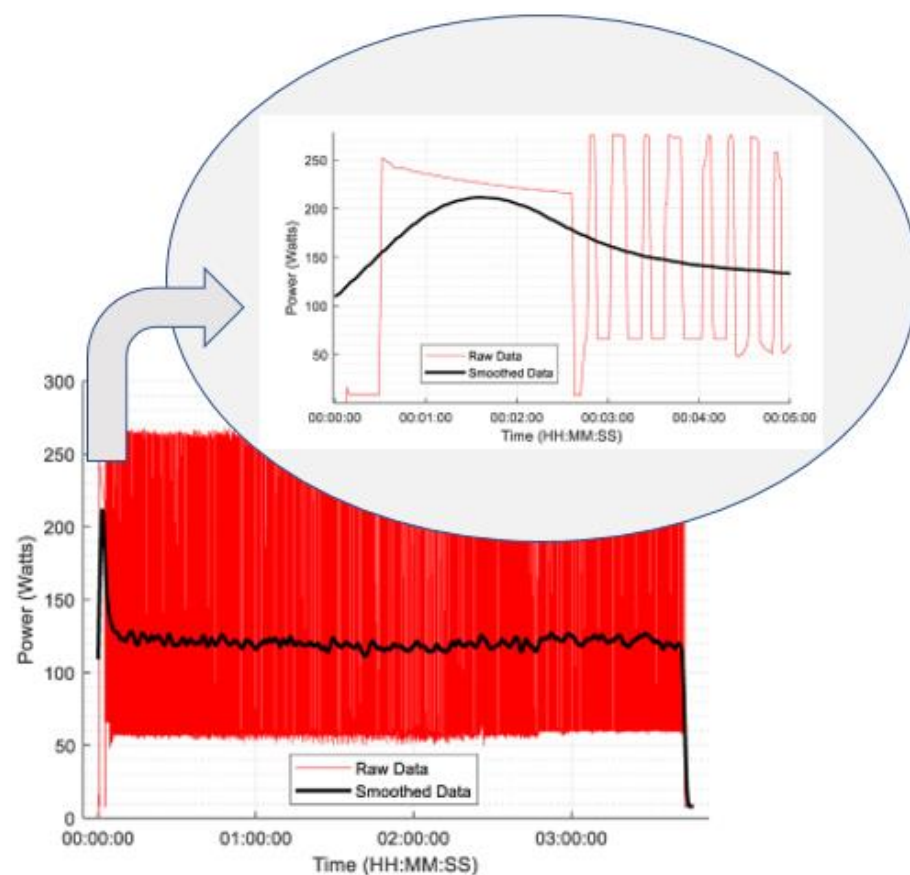
## 1. Introduction

Over the last decades, three-dimensional (3D) printing technology has been promising for small- and large-scale manufacturing technology. According to experts, the global 3D printing market is expected to reach a value of USD 57.1 billion by 2027. In addition to the development and increase in 3D technology, studies on the materials used in printing have increased and progressed. This naturally raises the issue of the efficiency of 3D printers. The efficiency of such printers can be scaled in regard to print time, power consumption, quality of the printing parts, etc. The parameters that affect them include calibration of the machine, nozzle temperature, bed temperature, ambient temperature, the speed of the print, and the orientation of the printing parts. Moreover, in metals, as in additive manufacturing, laser power and the preheating temperature of the powder bed can affect the relative density and mechanical properties of the parts [1,2]. The manufacturing process depends on the temperature of the nozzle, which is the end part of the machine providing flow for the fundamental base materials such as PLA, ABS, nylon, and PET. Due to the variation in their chemical composition, each material has different printing and decomposition temperatures, and they are provided in Table 1. Although most studies in the field of printing quality have generally focused on the materials, having different nozzle features affects the quality of the prints and the efficiency in terms of power consumption, too [3–7]. Another factor that affects the quality of a print is the nozzle's diameter [8]. Generally, brass, copper, and hardened steel are used for nozzles in 3D printers.

**Table 1.** Printing properties of the materials [3].

Material	Printing Temperature (°C)	Decomposition Temperature (°C)
ABS	230–250	380–430
PLA	200–235	300–400
Nylon	240–280	390–450
PET	160–210	350–480

Furthermore, increasing energy costs on a global scale has created a greater focus on energy efficiency; however, there is little current literature on the consumption of power by a 3D printer [9–11]. In a study by Hopkins, as shown in Figure 1, the measured power values for a printer during operation are given [9].

**Figure 1.** Power consumption of a printer during operation [9].

To understand the overall system's power consumption, it is necessary to understand which parts comprise the printer such as heated beds, controllers, motors and motor drivers, fans, LCD screens, filament, and nozzle. The breakdown of a specific printer's (i.e., Ender 3) energy consumption is given in Figure 2, where "hot end" refers to the nozzle. Although the energy used by the heated beds, motors, control boards, and fans change over time, generally, hot ends complete the process with constant temperatures, depending on the used material's features, as shown in Table 1. Hence, to provide the energy efficiency of the system, coating techniques were considered for different materials (i.e., brass, copper, and hardened steel). A thermal barrier coating (TBC) is an important technique that can be used to improve the lives of hot ends as well as to decrease the electricity used.

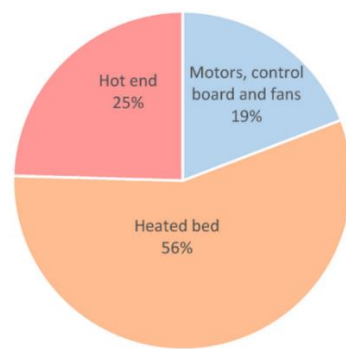


**Figure 2.** Distribution of the energy use of the printer [9].

The thermal barrier coating was used to protect parts operating at high temperatures due to the fact of its low thermal conductivity. Ceramic-based materials are mostly preferred as TBCs because of their resistance to high temperatures. Yttria-stabilized zirconia (YSZ) is used more commercially as a thermal barrier coating material. The acceptable thickness for a TBC is between 0.2 and 0.8 mm. It is used with a bond layer so that the TBC can adhere to the substrate's surface. In addition, the bond layer prevents oxidation and prolongs the service life of the part. YSZ has high thermal shock resistance and is used at operating temperatures up to 1200 °C. YSZ, of which the main material is zirconium, has low thermal conductivity. YSZ was chosen as the TBC in this study, and simulations were carried out using the thermal properties of YSZ, as they are preferred due to the fact of its easy accessibility and low thermal conductivity.

This paper aimed to address whether a TBC affects the energy efficiency of 3D printers. In accordance with this purpose, the TBC technique used is clearly explained and adapted to the nozzle in a simulated environment. In addition, by means of the finite element method (FEM), steady-state thermal analyses of the coated and uncoated nozzles were compared. This article also contributes a new topic to the literature in regard to comparisons of the efficiency between nozzles composed of three different materials and TBC models. As a result of the TBC method, it was found that the average heat flux was reduced, hence increasing the energy efficiency.

This paper had three main aims:

1. Performing steady-state thermal analyses for the specified materials by creating a nozzle model;
2. Assessing the effects of a TBC on the energy efficiency of various materials in the nozzle (i.e., brass, copper, and hardened steel) of the 3D printer;
3. Determination of the energy efficiency on the coating and uncoated nozzle with the TBC method.

#### *The Energy Required to Melt Filament in 3D Printing Technology*

The energy used to melt  $m$  kilograms of filament is given in Equation (1):

$$Q = mc(T_m - T_a) + mH_f \quad (1)$$

where:

- $Q$ : Energy (kJ);
- $m$ : Mass of the polymer (kg);
- $c$ : Specific heat capacity (kJ/kgK);
- $T_m$ : Polymer melting temperature (°C);
- $T_a$ : Ambient temperature (°C);
- $H_f$ : Heat of fusion (kJ/kg).

## 2. Materials and Simulation

### 2.1. Materials

In commercially used 3D printers, AHB is made of aluminum alloy. The reason for this is that it has good thermal conductivity and is an easily accessible material. The heat required for diffusion was applied to the AHB and transmitted to the nozzle. The printing temperatures are different, because different printing materials have different fusion temperatures. For this reason, nozzles are made of different materials depending on the diffusion temperatures of the material types. In addition, different materials are used in the manufacture of the nozzle in order to prevent abrasions in the nozzle. In this study, brass, copper, and hardened steel nozzles were used. The coated and uncoated CAD models of the AHB and nozzle used in the analyses are shown in Figure 3. In the analyses, YSZ was used as the thermal barrier coating. In order to use YSZ, it was determined to use NiCrAl as the bond layer [12–15]. After a literature review, the thickness of the bond layer was determined to be 0.15 mm and the TBC's thickness was determined as 0.5 mm. The physical properties of the materials used are also given in Table 2.

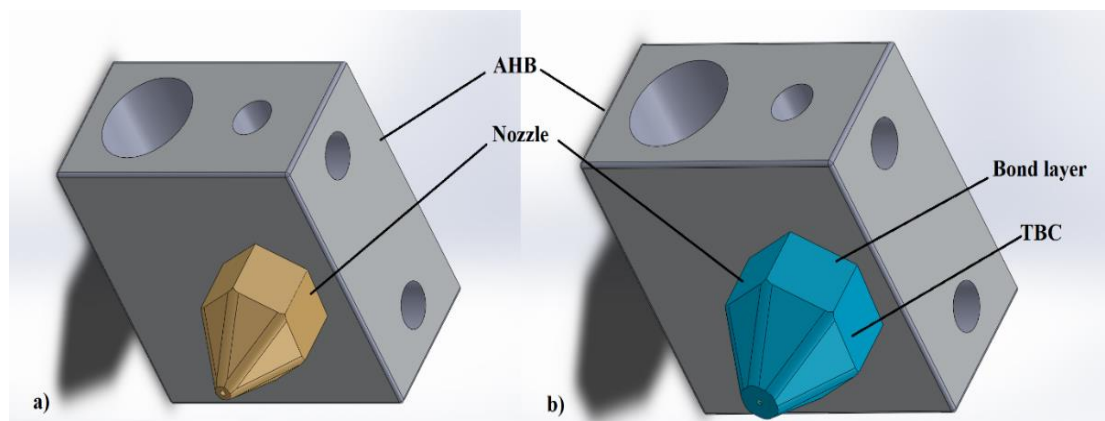


Figure 3. (a) AHB and nozzle CAD model; (b) coated CAD model.

Table 2. Thermal properties of the materials [16,17].

Material	Thermal Conductivity (W/m K)	Thermal Expansion $1 \times 10^{-6}$ (1/K)	Specific Heat (J/kg K)
Brass	105	19	0.380
Copper	330	16.4	0.385
Hardened Steel	22	14.8	0.55
Aluminum Alloy	114–175	22.8	0.873
NiCrAl	16.1	12	764
YSZ	2.2	10.9	620
La <sub>2</sub> Cr <sub>2</sub> O <sub>7</sub>	1.5	9.5	N/A

### 2.2. The Heat Transfer Model of the Nozzle

The heat transfer proceedings are usually solved depending on several assumptions. The use of these assumptions may not accurately reflect the processes encountered in the thermal engineering. In this study, the heat transfer model of the nozzle was addressed by means of Newton's law of cooling. Expressed in terms of temperature differences, Newton's law results in a simple differential equation that expresses the temperature difference as a function of time. The solution to this equation describes an exponential decrease in the temperature difference over time. This characteristic distortion of the temperature difference is also related to Newton's law of cooling and is expressed in Equation (2):

$$\frac{dT(t)}{dt} = -k(T(t) - T_{\infty}) \quad (2)$$

where:

$T(t)$ : Temperature at time  $t$ ;  
 $k$ : Temperature change coefficient;  
 $T_{\infty}$ : Environmental temperature.

Conduction, convection, and radiation are methods of heat transfer. In this study, heat transfer was addressed by conduction and convection. There is heat conduction between the layers of the AHB and the thermal barrier coating, and the equation describing this relationship is expressed in Equation (3):

$$Q_{cond} = kA(T_s - T_{\infty}) \quad (3)$$

where:

$A$ : Surface area through which the heat transfer takes place;  
 $T_s$ : Surface temperature.

Whether the AHBs are coated or uncoated, while in a non-flowing air environment, heat transfer is realized from its surfaces to the air as convection, and it is expressed by Equation (4):

$$Q_{conv} = hA(T_s - T_{\infty}) \quad (4)$$

where:

$h$ : Convection heat transfer coefficient.

### 2.3. Simulation of Finite Element Analysis

ANSYS is used to solve models that are decomposed into parts using the finite element method. It can analyze many systems, solving problems of strength, toughness, elasticity, deformations, heat transfer, fluid flow, electromagnetism, etc. In this study, steady-state thermal analyses were performed at the operating temperatures of the nozzles of the coated and uncoated models. While the uncoated model consisted of a nozzle and AHB, the coated model was additionally coated with a bond layer and a TBC. Heat transfer occurs between these layers when in contact with each other. Major heat transfer takes place by natural convection from the air-contacting surfaces of the AHB and nozzle. Boundary conditions used in the analysis:

- The operating temperatures of the nozzles made of various materials were different. In this study, the brass, copper, and hardened steel nozzles had maximum operating temperatures of 300, 500, and 450 °C, respectively. According to the type of material, the operating temperatures of the nozzles were applied from the socket of the heater cartridge of the AHB;
- The ambient air temperature that the models came into contact with was 22 °C. Due to the lack of air flow, the heat transfer from the model to the air occurred by natural convection, and the heat transfer coefficient was 5 W/m<sup>2</sup> K;
- The thermal properties of the bond layer and the TBC were used in the analyses as indicated in Table 1.

The mesh quality of all analyses were tested automatically using an option called convergence in ANSYS. For each analysis, the number of nodes and elements obtained as the result of mesh convergence are given graphically with the analysis results.

### 3. Results and Discussion

Steady-state thermal analyses were performed for the brass, copper, and hardened steel nozzles and the coated nozzles. Since the operating temperature and thermal properties of each nozzle were different, various results were obtained in the analyses. In all analyses, the heat was transferred by natural convection at the surfaces of the nozzles in contact with air, and the temperature distribution of the nozzles was calculated. The results of the coated and uncoated models were compared according to the type of material.

The maximum operating temperature of the brass nozzle was 300 °C. This temperature was applied to the AHB by the heater element and was one of the boundary conditions.

Considering this situation, the results of the thermal analysis of the nozzle made of brass are given in Figure 4. The results of the mesh convergence study of the uncoated brass nozzle are given in Figure 4e. Mesh convergence was automatically created in ANSYS, and the allowable change between mesh solutions was reduced to 5.5982%. While determining this value, the relationship between the solution time and the total heat flux was taken into account. The determined mesh structure was used in the analyses, and the mesh had 3,006,829 nodes and 2,169,395 elements. In Figure 4a, the total heat flux occurring on the surfaces of the model in contact with air is given. The average heat transfer per unit area was 13,745 W/m<sup>2</sup>. The temperature distribution of the nozzle is given in Figure 4c.

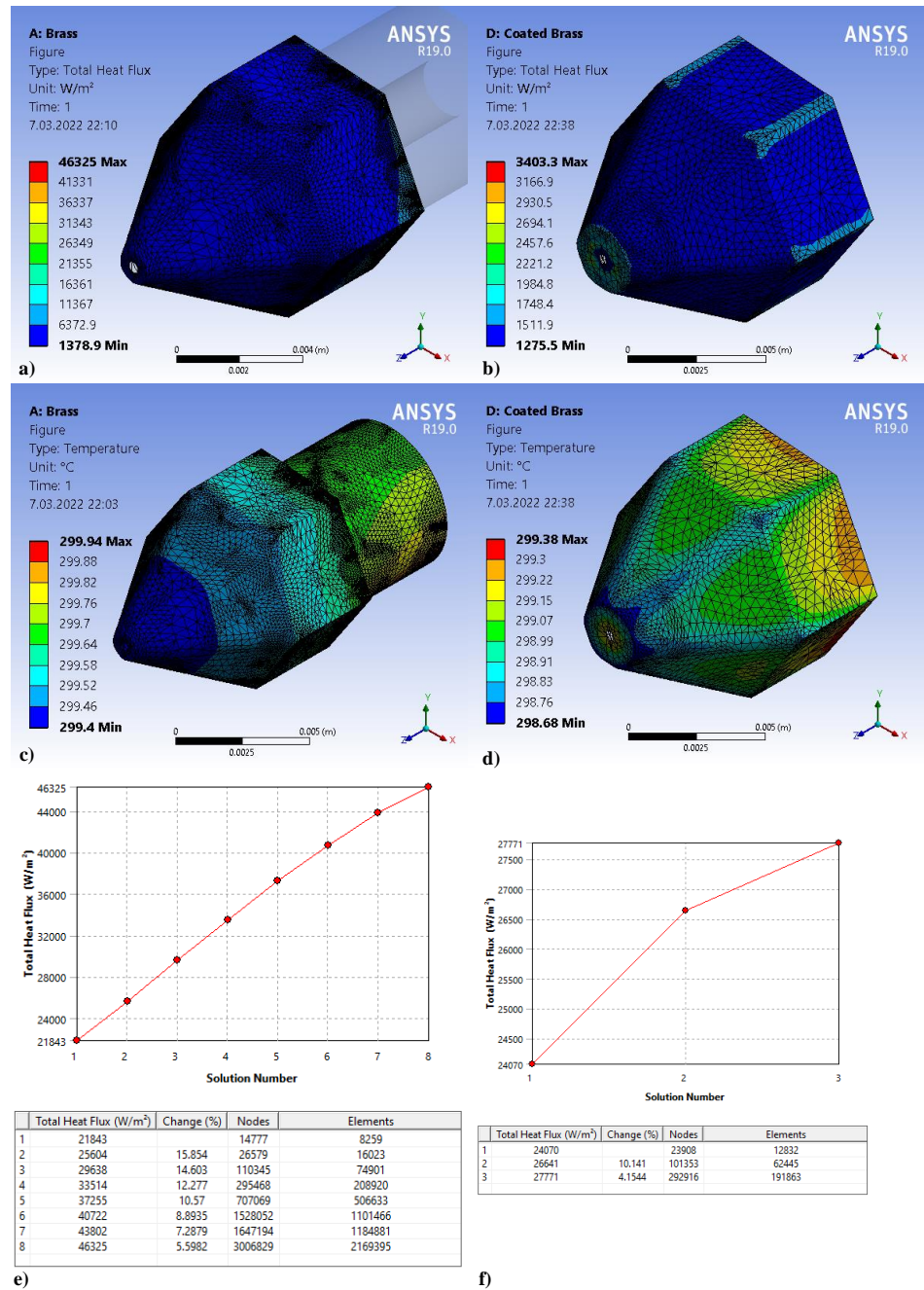


**Figure 4.** The total heat flux of (a) the brass nozzle and (b) the coated brass nozzle; temperature distribution of (c) the brass nozzle and (d) the coated brass nozzle; mesh convergence study based on the total heat flux of (e) the brass nozzle and (f) the coated brass nozzle.

As seen in Figure 4f, the allowable change was reduced to 4.1544% in the mesh convergence study on the coated brass nozzle. The mesh structure contained 292,916 nodes and 191,863 elements. The total heat flux analysis of the coated brass nozzle is given in Figure 4b. The average heat flux was found to be 1453.9 W/m<sup>2</sup>. The temperature distribution of the coated nozzle is shown in Figure 4d.

In Reference [4], the effect of the TBC on the energy efficiency in additive manufacturing was investigated. Numerical analyses showed that energy efficiency can be achieved by increasing the thermal efficiency using the TBC method. In this study, when the coated and uncoated brass nozzle models were compared, it was observed that the average heat flux per unit area by convection decreased by 89.4223%. The average nozzle temperature decreased by 0.68 °C. By reducing the heat flux into the environment, the loss of energy in the form of heat was prevented.

The copper nozzle had a maximum operating temperature of 500 °C. The high operating temperature and thermal conductivity of the copper nozzle led to the striking analysis results. The steady-state thermal analysis of the copper nozzle is given in Figure 5. As shown in Figure 5e, the uncoated model was divided into 2,585,993 nodes and 1,853,244 elements as a result of the mesh convergence study. The total heat flux is given in Figure 5a, and the average heat flux was 33,571 W/m<sup>2</sup>. Due to the high thermal conductivity of copper, the average heat flux transferred into the environment by natural convection was high. The temperature distribution over the uncoated nozzle is shown in Figure 5c, and the mesh structure of the model can also clearly be seen in the figure.

The mesh convergence study of the coated copper nozzle approached zero in the eleventh solution, as shown in Figure 5f, and the mesh structure included 1,108,779 nodes and 784,351 elements. The total heat flux of the coated model is given in Figure 5b, and the average heat flux was 2797.2 W/m<sup>2</sup>. The temperature distribution of the TBC on the copper nozzle is given in Figure 5d.

Applying the TBC to the copper nozzle reduced the average heat flux per unit area on the nozzle by 91.6678%. According to the literature, it is possible to reduce the surface temperature of the parts with a thermal barrier coating [18]. Due to this phenomenon, the TBC lowered the average temperature of the nozzle by 0.88 °C. Lowering the average temperature contributed positively to reducing the heat transfer due to the temperature difference.

Hardened steel is a medium or high carbon steel that has been heat treated. Abrasions occurring in brass nozzles are minimized in nozzles produced from hardened steel. It is used in printing processes of filaments, such as carbon fiber, at a maximum operating temperature of 450 °C. The maximum operating temperature was used in the analyses. The results of the analysis of the coated and the uncoated hardened steel nozzle are given in Figure 6. Mesh convergence studies for both models are shown in Figure 6e,f. The uncoated nozzle was divided into 2,159,011 nodes and 1,532,149 elements, and the coated nozzle was divided into 1,581,931 nodes and 1,137,488 elements. In Figure 6a, the total heat flux of the uncoated nozzle is given, and the average heat flux was found to be 13,371 W/m<sup>2</sup>. The total heat flux of the coated nozzle is shown in Figure 6b. The average heat flux in the TBC nozzle was 2789.7 W/m<sup>2</sup>. The average heat flux from the unit area into the environment was reduced by 79.1361% due to the TBC. The temperature distributions for both models are given in Figure 6c,d. While the average temperature of the coated nozzle was 446.72 °C, the average temperature of the uncoated nozzle was calculated as 448.99 °C. The TBC reduced the nozzle temperature by 2.27 °C.

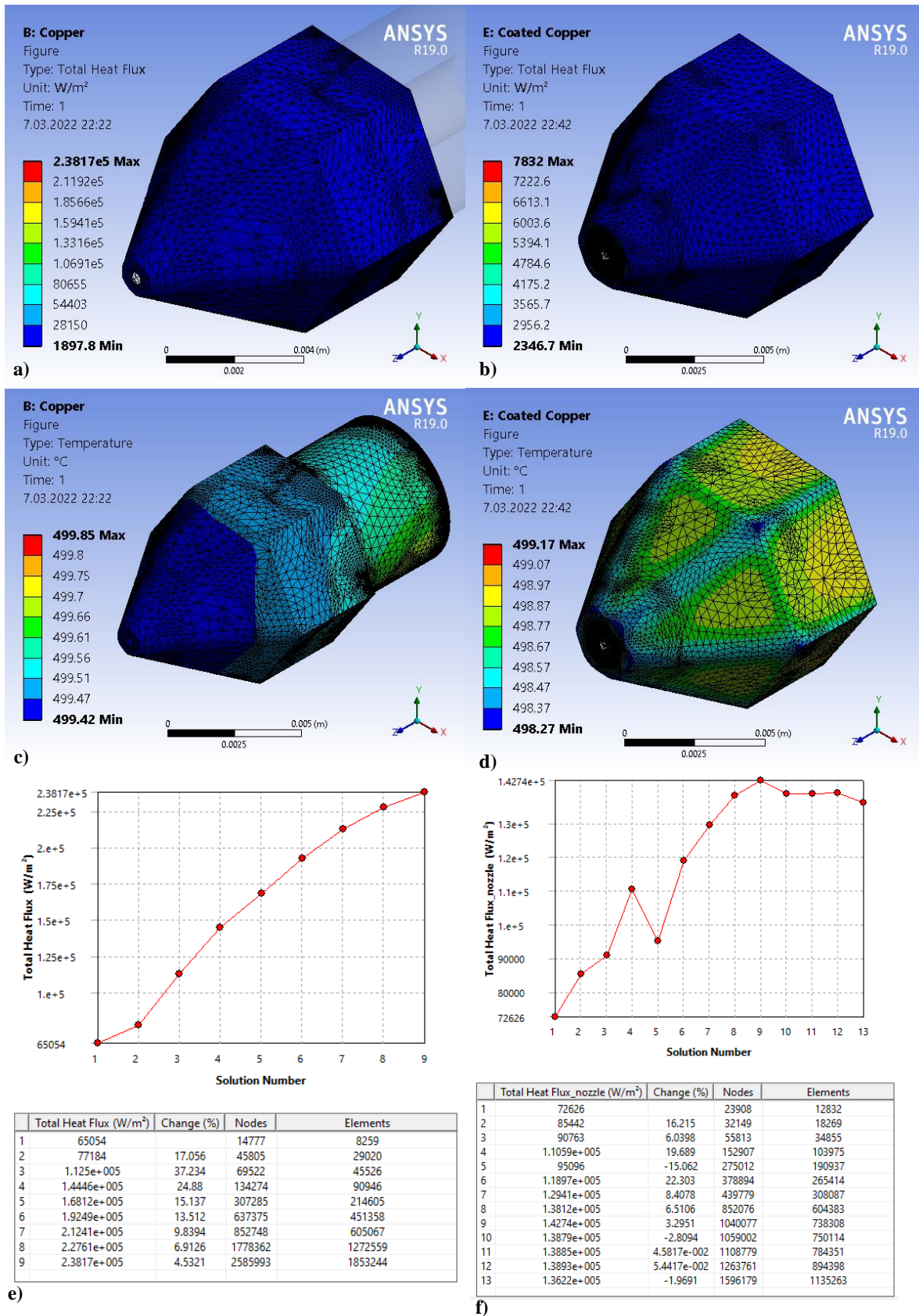


**Figure 5.** The total heat flux of (a) the copper nozzle and (b) coated copper nozzle; temperature distribution of (c) the copper nozzle and (d) the coated copper nozzle; mesh convergence study based on the total heat flux of (e) the copper nozzle and (f) the coated copper nozzle.

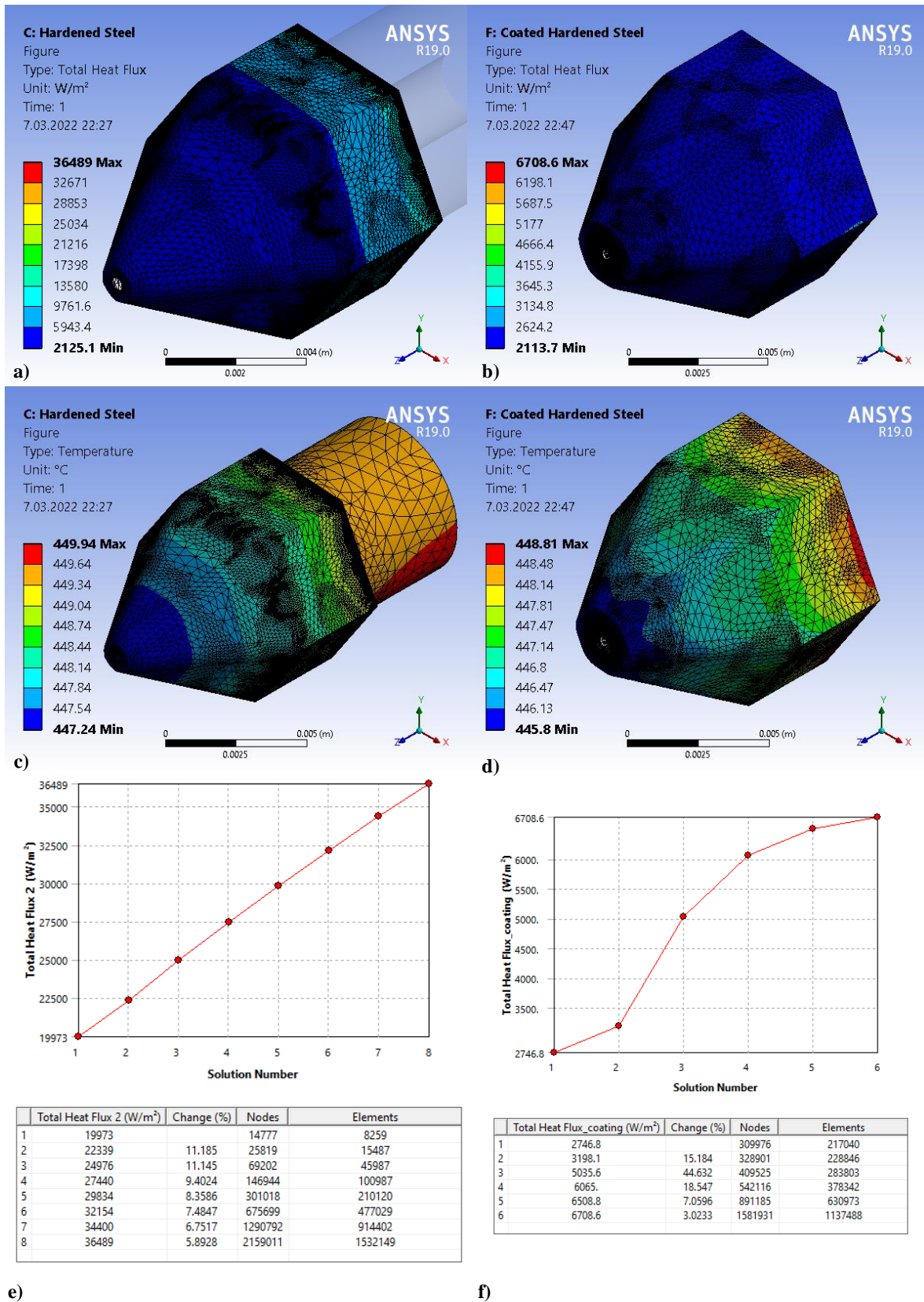


**Figure 6.** The total heat flux of (a) the hardened steel nozzle and (b) the coated hardened steel nozzle; temperature distribution of (c) the hardened steel nozzle and (d) the coated hardened steel nozzle; mesh convergence study based on the total heat flux of (e) the hardened steel nozzle and (f) the coated hardened steel nozzle.

To conclude the numerical simulations, the average heat flux plot obtained for the three material types in the analyses is given in Figure 7. Although the energy losses were reduced at the same rate in all the materials, the decrease in the average heat flux was greater in the nozzle made of copper. The application of the TBC to the copper nozzle increased the energy gain more than the other nozzles. This was due to the high thermal conductivity of copper and the high operating temperature of the copper nozzle. The TBC reduced heat losses in all nozzle types. By reducing losses, energy efficiency was increased, which will lead to lower costs.

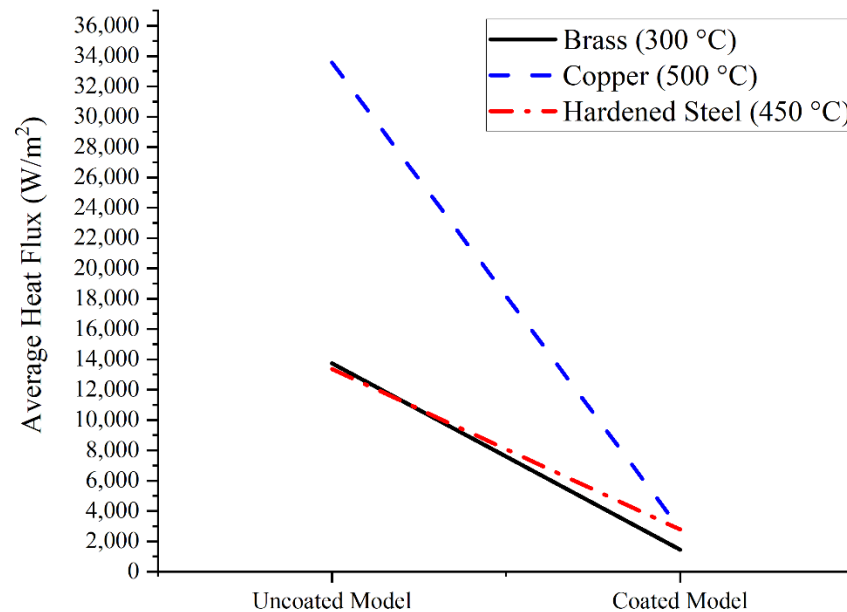


**Figure 7.** The average heat flux of the coated and uncoated models.

#### 4. Conclusions

In this study, steady-state thermal analyses of nozzles made of three different materials and models made of a TBC were performed to increase the energy efficiency. The TBC method, which is composed of materials with low thermal conductivity, reduced the thermal conductivity and the energy losses. As a result of the analyses, the following findings were reached:

- The TBC method greatly reduced the amount of heat transferred into the environment, preventing energy losses and increasing energy efficiency. The applicability of the TBC method in 3D printers has been demonstrated in the literature, and it is clear that it will increase the thermal efficiency;
- It was found that the average heat flux was greatly reduced by applying a TBC to nozzles made of brass, copper, and hardened steel;
- Although the energy efficiency of the copper nozzle was the same rate as the other nozzles, there was a numerically higher energy efficiency than the other nozzles. This is because copper has a high thermal conductivity coefficient, and the operating temperature of the copper nozzle was higher than the other nozzles. If the difference between the ambient temperature and the operating temperature was large, the heat flow will increase according to the theory of heat transfer by convection. The TBC prevented heat loss and provided high energy efficiency;
- Reducing energy losses will cause the heater element to work less. This will contribute to energy efficiency by reducing the energy consumption used for heating.

The finite element analysis showed that the TBC method dramatically reduced energy loss through the nozzle. It was found that the average heat flux was reduced by 89.4223% in the brass nozzle, 91.6678% in the copper nozzle, and 79.1361% in the hardened steel

nozzle. Increasing the thermal efficiency by reducing thermal permeability increased energy efficiency, as it reduced the energy losses.

**Author Contributions:** Conceptualization, methodology, investigation, writing original draft: A.E.C.; software, formal analysis, data curation, visualization, project administration, H.D.; investigation, resources, writing—original draft preparation, writing—review and editing, supervision, H.D. and A.E.C. All authors have read and agreed to the published version of the manuscript.

**Funding:** This research received no external funding.

**Institutional Review Board Statement:** Not applicable.

**Informed Consent Statement:** Not applicable.

**Data Availability Statement:** Not applicable.

**Conflicts of Interest:** The authors declare no conflict of interest.

## References

1. Luo, X.; Yang, C.; Fu, Z.Q.; Liu, L.H.; Lu, H.Z.; Ma, H.W.; Wang, Z.; Li, D.D.; Zhang, L.C.; Li, Y.Y. Achieving Ultrahigh-Strength in Beta-Type Titanium Alloy by Controlling the Melt Pool Mode in Selective Laser Melting. *Mater. Sci. Eng. A* **2021**, *823*, 141731. [CrossRef]
2. Luo, X.; Liu, L.H.; Yang, C.; Lu, H.Z.; Ma, H.W.; Wang, Z.; Li, D.D.; Zhang, L.C.; Li, Y.Y. Overcoming the Strength–Ductility Trade-off by Tailoring Grain-Boundary Metastable Si-Containing Phase in  $\beta$ -Type Titanium Alloy. *J. Mater. Sci. Technol.* **2021**, *68*, 112–123. [CrossRef]
3. Wojtyła, S.; Klama, P.; Baran, T. Is 3D Printing Safe? Analysis of the Thermal Treatment of Thermoplastics: ABS, PLA, PET, and Nylon. *J. Occup. Environ. Hyg.* **2017**, *14*, D80–D85. [CrossRef] [PubMed]
4. Demir, H. The Effects on Thermal Efficiency of Yttria-Stabilized Zirconia and Lanthanum Zirconate-Based Thermal Barrier Coatings on Aluminum Heating Block for 3D Printer. *Coatings* **2021**, *11*, 792. [CrossRef]
5. Veselý, P. Nozzle temperature effect on 3d printed structure properties. In Proceedings of the Elektrotechnológia 2019, Zuberec, Slovakia, 21–23 May 2019; Volume 7.
6. Demir, H.; Coşgun, A.E. 3B Yazıcılarda Kullanılan Farklı Tip Ekstüderlerin ANSYS Programı ile Termal Analizlerinin Gerçekleştirilmesi. *Diğce Üniversitesi Bilim Teknol. Derg.* **2021**, *10*, 275–284. [CrossRef]
7. Demir, H.; Coşgun, A.E. Comparison of PLA and ABS on Robot Arm Model and 3D Technology. *Eur. J. Adv. Eng. Technol.* **2019**, *6*, 38–44.
8. Czyżewski, P.; Marciniak, D.; Nowinka, B.; Borowiak, M.; Bieliński, M. Influence of Extruder's Nozzle Diameter on the Improvement of Functional Properties of 3D-Printed PLA Products. *Polymers* **2022**, *14*, 356. [CrossRef] [PubMed]
9. Hopkins, N.; Jiang, L.; Brooks, H. Energy Consumption of Common Desktop Additive Manufacturing Technologies. *Clean. Eng. Technol.* **2021**, *2*, 100068. [CrossRef]
10. Rejeski, D.; Zhao, F.; Huang, Y. Research Needs and Recommendations on Environmental Implications of Additive Manufacturing. *Addit. Manuf.* **2018**, *19*, 21–28. [CrossRef]
11. Yang, Y.; Li, L.; Pan, Y.; Sun, Z. Energy Consumption Modeling of Stereolithography-Based Additive Manufacturing toward Environmental Sustainability. *J. Ind. Ecol.* **2017**, *21*, 12589. [CrossRef]
12. Kushwaha, A.K.; Mishra, S.P.; Vishwakarma, M.K.; Chauhan, S.; Jappor, H.R.; Khenata, R.; Omran, S. Bin Theoretical Study of Thermal Conductivity, Mechanical, Vibrational and Thermodynamical Properties of  $\text{Ln}_2\text{Zr}_2\text{O}_7$  ( $\text{Ln} = \text{La}, \text{Nd}, \text{Sm}, \text{and Eu}$ ) Pyrochlore. *Inorg. Chem. Commun.* **2021**, *127*, 108495. [CrossRef]
13. Hayashi, H.; Saitou, T.; Maruyama, N.; Inaba, H.; Kawamura, K.; Mori, M. Thermal Expansion Coefficient of Yttria Stabilized Zirconia for Various Yttria Contents. *Solid State Ion.* **2005**, *176*, 613–619. [CrossRef]
14. Itoh, Y.; Saitoh, M. Mechanical Properties of Overaluminized MCrAlY Coatings at Room Temperature. *J. Eng. Gas Turbines Power* **2005**, *127*, 807–813. [CrossRef]
15. Khaloobagheri, M.; Janipour, B.; Askari, N.; Shafiee Kamal Abad, E. Characterisation of Powder Metallurgy Cu-ZrO<sub>2</sub> Composites. *Adv. Prod. Eng. Manag.* **2013**, *242–248*. [CrossRef]
16. Manohar, B.; Jothi, M.; Rajamanickam, U. The Effects of Thermal Barrier Coating on Thermal Stress and Temperature Distribution in a Diesel Engine Piston for Magnesia/Yittria Partially Stabilized Zirconia. *IJRMET* **2016**, *6*, 8.
17. Online Materials Information Resource. MatWeb. Available online: <https://www.matweb.com/index.aspx> (accessed on 1 May 2022).
18. Singh, G.; Bala, N.; Mishra, A. Comprehensive Review on MCrAlY Coatings: Structure, Properties and Future. *Int. J. Adv. Sci. Technol.* **2020**, *29*, 4867–4870.